Korean J. Chem. Eng., 34(1), 206-213 (2017)
DOI: 10.1007/s11814-016-0247-7

pISSN: 0256-1115
eISSN: 1975-7220

Solubility and dissolution thermodynamics of hexaquoiron(III)tris(*p*-toluenesulfonate) in (ethanol+water) binary mixtures within 291.15-333.15 K

Zhijuan Huang, Chao Yu, Weilan Xue, Fucong Lin, and Zuoxiang Zeng†

Institute of Chemical Engineering, East China University of Science and Technology, Shanghai 200237, China

(*Received 5 May 2016 • accepted 29 August 2016*)

Abstract−The solubility of hexaquoiron(III)tris(*p*-toluenesulfonate) [$Fe(OTs)_3{\cdot}6H_2O$] in (ethanol+water) mixtures with a mole fraction of 0-0.327 ethanol was measured from 291.15 to 333.15 K by using a synthetic method. The experimental results show that the solubility of $Fe(OTs)_3{\cdot}6H_2O$ increases with an increase in temperature and an enrichment in ethanol content. The solubility data were correlated by the modified Apelblat equation, the Redlich-Kister (CNIBS/R-K) model, and the hybrid model, and the results showed that the three models agree well with experimental data. The thermodynamic properties of the dissolution process, including enthalpy, entropy, and Gibbs energy were estimated from the experimental data by the modified van't Hoff equation, indicating that the process of the dissolution of $Fe(OTs)_3{\cdot}6H_2O$ is endothermic and spontaneous.

Keywords: Hexaquoiron(III)tris(*p*-toluenesulfonate), Thermodynamics, Correlation, Solubility, Phase Equilibria

INTRODUCTION

Hexaquoiron(III)tris(*p*-toluenesulfonate) [$Fe(OTs)_3{\cdot}6H_2O$, $C_{21}H_{33}FeO_{15}S_3$, CAS Registry No. 312619-41-3] is an orange crystalline solid. Its structural formula is shown in Fig. 1. It is widely used as an effective catalyst for many reactions [1-6]. For example, $Fe(OTs)_3{\cdot}6H_2O$ is an effective catalyst for the intramolecular hydroalkoxylation of unactivated alkenes, the intermolecular hydroalkoxylation of styrene, and the hydrocarboxylation and hydroalkynylation of norbornene [3-6]. In addition, it is an efficient, inexpensive, easy to handle, and available catalyst for the deprotection of *tert*-butyldimethylsiltyl, triethoxysilane and triisopropylsilyl ethers [7]. What's more, $Fe(OTs)_3{\cdot}6H_2O$ is the catalyst for the deprotection of a wide range of aromatic acetals in water [8].

Ethanol and water are usually used as the solvents for many organic reactions when $Fe(OTs)_3{\cdot}6H_2O$ works as catalyst [6,8]. The solubility of solute is important to design an optimized production process. However, the solubility of $Fe(OTs)_3{\cdot}6H_2O$ in (ethanol+water) binary mixtures has not been reported in the literature.

In this study, we used synthetic method to determine the solubility of $Fe(OTs)_3{\cdot}6H_2O$ in (ethanol+water) binary mixtures with different mole fractions of ethanol (0, 0.050, 0.099, 0.147, 0.193, 0.239, 0.285, 0.327) from T=(291.15 to 333.15) K under atmospheric pressure. The experimental solubility data were correlated with the modified Apelblat model, the Redlich-Kister (CNIBS/R-K) model, and the hybrid model. Meanwhile, the enthalpy (ΔH^0_{soln}), the entropy (ΔS^0_{soln}) and the molar Gibbs free energy (ΔG^0_{soln}) of the dissolution process were calculated by the modified van't Hoff equation.

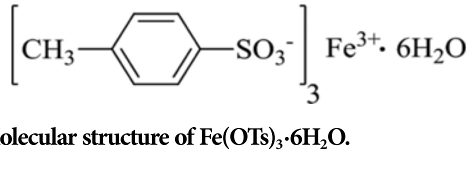

Fig. 1. Molecular structure of $Fe(OTs)_3{\cdot}6H_2O$.

EXPERIMENTAL SECTION

1. Materials

$Fe(OTs)_3{\cdot}6H_2O$ (purity>99.0 mass%) was prepared in our laboratory according to the method in literature [9], and its purity was measured by high performance liquid chromatography (HPLC). The thermal gravity analysis (TGA) was carried out on TGA/SDTA851, Mettler Instrument Inc. with a heating rate of 10 K·min^{-1} from 298.15 to 1,073.15 K. The flow rate of nitrogen gas was 50 mL·min^{-1},

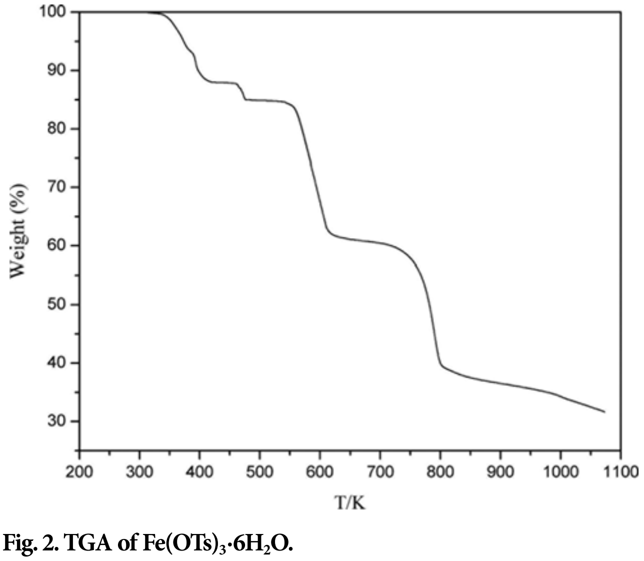

Fig. 2. TGA of $Fe(OTs)_3{\cdot}6H_2O$.

---

†To whom correspondence should be addressed.
E-mail: zengzx@ecust.edu.cn

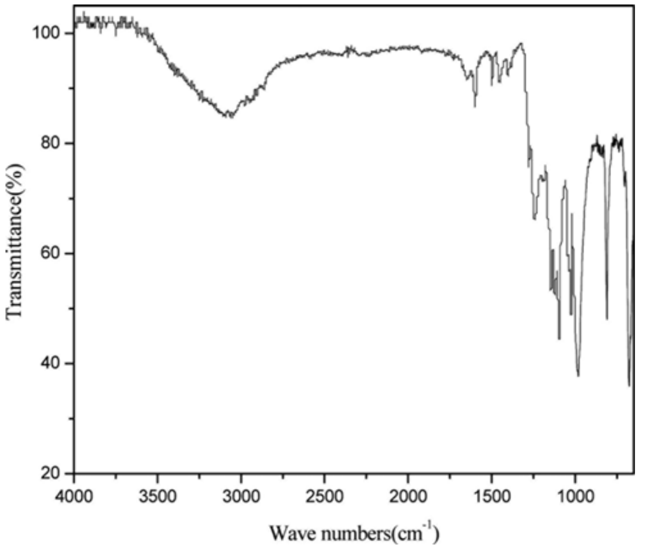

Fig. 3. IR spectrum of $Fe(OTs)_3·6H_2O$.

and the mass of TGA sample was about 10.000 mg. The dehydration temperature was determined to be accurate to ±0.1 K. The thermal analysis result of $Fe(OTs)_3·6H_2O$ is shown in Fig. 2. It can be seen that the first five water of crystallization in $Fe(OTs)_3·6H_2O$ decreases at ~408 K, and the last one at ~465 K. IR spectra were recorded in the 4,000-400 cm^{-1} range as KBr pellets on Nexus 670, which was supplied by Thermo Electron Corporation, USA (shown in Fig. 3). The absorption band images of the energy disperse spectroscope of $Fe(OTs)_3·6H_2O$ are shown in Supporting Information (SI) Fig. S1. Anal. calcd. for $C_{21}H_{33}FeO_{15}S_3$: C, 37.23; O, 35.42; S, 14.20; Fe, 8.24. Found: C, 37.21; O, 35.40; S, 14.10; Fe, 8.22. Ethanol with purity of 99.7% was supplied by Shanghai TiTan Scientific Co., Ltd.

2. Solubility Measurement

In this work, the solubility of $Fe(OTs)_3·6H_2O$ in (ethanol+water) binary mixtures was determined by the last crystal disappearance method, which is one type of synthetic method [10,11]. The crystal water in solute will become a part of the solvent during the dissolving process to change the composition of solvent. To make the final mole fractions of ethanol of the binary mixtures be the same (0, 0.050, 0.099, 0.147, 0.193, 0.239, 0.285, 0.327) at different temperatures, the initial mole fractions of ethanol of the binary mixtures were determined by the pre-experiment described in SI. The procedure of the experiment was as follows. First, a certain mass (20±0.001 g) of solvent mixtures with an initial mole fraction of ethanol (x_2^0, shown in the SI) was added into a three-necked flask that was maintained at the desired temperature (*T*) by a cylindrical glass thermostatic water bath (SYP-D, Jintan Guowang Experimental Instrument Factory, Changzhou, China). The solution temperature was measured by a mercury thermometer (fluctuates within ±0.05 K). A magnetic stirrer was used to mix the suspensions. To prevent the evaporation of the solvent at high temperature, a reflux condenser was also used. Then a known amount of $Fe(OTs)_3·6H_2O$ weighted by an analytical balance (Mettler H542, uncertainty of 0.0001 g) was added to the three-necked flask at the temperature. The next proper of solid (less than 0.05 g) was added to the vessel when the former solid increment had completely dissolved. The above process was repeated until the last increment (less than 0.01 g) remained partially undissolved for 2 h. All the experiments were conducted at least three times, and the average values were used to calculate the mole fraction solubility. The mole fraction solubility of $Fe(OTs)_3·6H_2O$ (x_1) was obtained by Eq. (1). The final mole fraction of ethanol in the solvent mixture (x_2) can be calculated according to Eq. (2):

$$x_1=\frac{m_1/M_1}{7\times m_1/M_1+m_2/M_2+m_3/M_3} \tag{1}$$

$$x_2=\frac{m_2/M_2}{6\times m_1/M_1+m_2/M_2+m_3/M_3} \tag{2}$$

where m_1, m_2, and m_3 are the mass of the $Fe(OTs)_3·6H_2O$, ethanol, and water, respectively [12]. M_1, M_2, and M_3 are the molecular mass of $Fe(OTs)_3·6H_2O$, ethanol, and water, respectively. The uncertainties of temperature fluctuation of the water bath, temperature measurements, and weighing procedure may cause the uncertainty of solubility measurement of $Fe(OTs)_3·6H_2O$, which is no more than 2.0%.

RESULTS AND DISCUSSION

1. Data Correlation

To investigate the relationship of x_1-T-x_2, the modified Apelblat equation, the Redlich-Kister (CNIBS/R-K) model, and the hybrid model were adopted. The parameters of these models were calculated by least square method.

1-1. Modified Apelblat Equation

The modified Apelblat equation, which describes the relationship between x_1 and T, is given as follows [13,14]:

$$\ln(x_1)=a+\frac{b}{T}+c\ln T \tag{3}$$

where a, b and c are the model parameters. The values of a and b reflect the variation of the influence of solution nonidealities on the solubility of solute, and the value of c represents the effect of temperature on the enthalpy of fusion.

1-2. Redlich-Kister (CNIBS/R-K) Model

The Redlich-Kister (CNIBS/R-K) model is a theoretical model which describes the relationship between x_1 and x_2. It is represented in Eq. (4) [15]:

$$\ln(x_1)=x_2^B\ln(x_1)_{B.T}+x_2^C\ln(x_1)_{C.T}+x_2^Bx_2^C\sum_{i=0}^{n}S_i(x_2^B-x_2^C)^i \tag{4}$$

where x_2^B (or x_2^C) refers to the mole fraction of ethanol (or water) when the solute is not added. $(x_1)_{B.T}$ (or $(x_1)_{C.T}$) is the mole fraction of the solute in ethanol (or water) at temperature T. S_i is the model constant and n is the number of the solvents. In this experiment, n=2. x_2^C is substituted with $1-x_2^B$, and Eq. (4) can be written as follows:

$$\begin{aligned}\ln(x_1)=&[\ln(x_1)_{B.T}-\ln(x_1)_{C.T}+S_0-S_1+S_2]x_2^B+(-S_0+3S_1-5S_2)(x_2^B)^2\\&+(-2S_1+8S_2)(x_2^B)^3+(-4S_2)(x_2^B)^4+\ln(x_1)_{C.T}\end{aligned} \tag{5}$$

Eq. (5) can be simplified as Eq. (6)

$$\ln(x_1)=A_1+A_2x_2^B+A_3(x_2^B)^2+A_4(x_2^B)^3+A_5(x_2^B)^4 \tag{6}$$

where A_1, A_2, A_3, A_4 and A_5 are the model parameters.

1-3. Hybrid Model

The hybrid model is used to describe the influence of both the composition of the solvent and the temperature on the solubility data, and can be written as Eq. (7) [16].

$$\ln(x_1)=x_2^B\ln(x_1)_{B.T}+x_2^C\ln(x_1)_{C.T}+x_2^Bx_2^C\sum_{i=0}^{n}\frac{J_i(x_2^B-x_2^C)^i}{T} \tag{7}$$

where J_i is the model parameter, and the other symbols donate the same meaning as Eq. (4). According to Eq. (3), $\ln(x_1)_{B.T}$ and $\ln(x_1)_{C.T}$ can be expressed as the following:

$$\ln(x_1)_{B.T}=a_1+\frac{b_1}{T}+c_1\ln T \tag{8}$$

$$\ln(x_1)_{C.T}=a_2+\frac{b_2}{T}+c_2\ln T \tag{9}$$

In this work, n=2 and substituting x_2^C with $1-x_2^B$, Eq. (7) can be written as Eq. (10)

$$\begin{aligned}\ln(x_1)=&\,a_1+\frac{b_1}{T}+c_1\ln T+(a_1-a_2)x_2^B+(b_1-b_2+J_0-J_1+J_2)\frac{x_2^B}{T}\\&+(-J_0+3J_1-5J_2)\frac{(x_2^B)^2}{T}+(-2J_1+8J_2)\frac{(x_2^B)^3}{T}\\&+(-4J_2)\frac{(x_2^B)^4}{T}+(c_1-c_2)x_2^B\ln T\end{aligned} \tag{10}$$

Solving simultaneously Eqs. (8)-(10), the hybrid model equation will be obtained as Eq. (11) [17].

$$\begin{aligned}\ln(x_1)=&\,B_1+\frac{B_2}{T}+B_3\ln T+B_4x_2^B+B_5\frac{x_2^B}{T}+B_6\frac{(x_2^B)^2}{T}\\&+B_7\frac{(x_2^B)^3}{T}+B_8\frac{(x_2^B)^4}{T}+B_9x_2^B\ln T\end{aligned} \tag{11}$$

in which, B_1 to B_9 are the model parameters.

2. Solubility Data of $Fe(OTs)_3\cdot6H_2O$

The experimental solubility data of $Fe(OTs)_3\cdot6H_2O$ shown in Table 1 were correlated with Eqs. (3), (6), and (11), and the parameters of the above models are listed in Tables 2-4. The comparisons between experimental data and calculated ones are also presented in

Table 1. Experimental and calculated solubilities of $Fe(OTs)_3\cdot6H_2O$ in (ethanol+water) binary mixtures at temperature *T* and pressure *p*= 0.1 MPa

T/K	$10^3x_1^{exp}$	$(x_1^{exp}-x_1^{cal})/x_1^{exp}$			$10^3x_1^{exp}$	$(x_1^{exp}-x_1^{cal})/x_1^{exp}$		
		Apelblat	CNIBS/R-K	Hybrid		Apelblat	CNIBS/R-K	Hybrid
		$x_2=0$				$x_2=0.050$		
291.15	10.71	−0.0282	0.0009	−0.0759	13.11	−0.0084	−0.0042	−0.0200
295.15	12.56	0.0400	−0.0032	0.0071	14.67	0.0240	0.0092	0.0212
299.15	13.26	0.0074	−0.0011	−0.0158	15.35	−0.0083	0.0016	−0.0044
303.15	14.21	−0.0099	−0.0013	−0.0241	16.38	−0.0190	0.0017	−0.0100
306.15	15.11	−0.0113	−0.0041	−0.0191	17.81	0.0091	0.0150	0.0205
309.15	16.38	0.0073	−0.0025	0.0052	18.47	−0.0088	0.0060	0.0046
313.15	17.36	−0.0162	−0.0051	−0.0116	20.20	0.0098	0.0174	0.0241
316.15	18.88	0.0079	−0.0039	0.0166	21.25	0.0090	0.0139	0.0232
319.15	19.68	−0.0092	−0.0027	0.0034	21.98	−0.0081	0.0072	0.0054
323.15	21.64	0.0086	−0.0024	0.0250	23.64	−0.0015	0.0081	0.0096
326.15	22.92	0.0092	−0.0012	0.0281	25.09	0.0091	0.0037	0.0176
329.15	23.83	−0.0077	−0.0032	0.0136	25.87	−0.0076	0.0100	−0.0022
333.15	25.85	0.0007	−0.0005	0.0239	27.76	0.0006	0.0007	0.0006
		$x_2=0.099$				$x_2=0.147$		
291.15	15.74	0.0029	0.0124	0.0373	17.20	0.0103	−0.0190	0.0260
295.15	16.40	−0.0096	−0.0013	0.0143	17.65	−0.0115	−0.0218	−0.0065
299.15	17.55	0.0032	0.0113	0.0174	18.55	−0.0117	−0.0298	−0.0160
303.15	18.69	0.0092	0.0074	0.0153	19.94	0.0088	−0.0209	−0.0030
306.15	19.17	−0.0089	−0.0135	−0.0080	20.76	0.0086	−0.0072	−0.0078
309.15	20.42	0.0100	0.0071	0.0066	21.28	−0.0080	−0.0300	−0.0286
313.15	21.34	−0.0060	−0.0137	−0.0144	22.69	−0.0005	−0.0147	−0.0248
316.15	22.34	−0.0058	−0.0133	−0.0171	23.97	0.0106	−0.0037	−0.0153
319.15	23.80	0.0111	0.0043	−0.0021	24.64	−0.0063	−0.0258	−0.0339
323.15	24.82	−0.0101	−0.0056	−0.0255	26.21	−0.0052	−0.0081	−0.0331
326.15	26.51	0.0082	−0.0032	−0.0076	27.87	0.0098	−0.0022	−0.0172
329.15	27.30	−0.0109	−0.0055	−0.0271	28.71	−0.0078	−0.0143	−0.0341
333.15	29.65	0.0063	0.0019	−0.0089	30.91	0.0017	−0.0087	−0.0217

Table 1. Continued

T/K	$10^3x_1^{exp}$	$(x_1^{exp}-x_1^{cal})/x_1^{exp}$			$10^3x_1^{exp}$	$(x_1^{exp}-x_1^{cal})/x_1^{exp}$		
		Apelblat	CNIBS/R-K	Hybrid		Apelblat	CNIBS/R-K	Hybrid
		$x_2=0.193$				$x_2=0.239$		
291.15	19.23	0.0044	0.0145	0.0571	19.89	0.0161	−0.0046	0.0221
295.15	19.71	−0.0104	0.0224	0.0302	20.32	−0.0121	0.0008	−0.0036
299.15	20.87	0.0042	0.0217	0.0334	21.51	−0.0053	0.0034	0.0047
303.15	21.89	0.0067	0.0152	0.0266	22.44	−0.0133	0.0035	−0.0026
306.15	22.31	−0.0099	0.0085	0.0046	23.65	0.0009	0.0128	0.0115
309.15	23.58	0.0083	0.0170	0.0176	24.65	0.0043	0.0166	0.0143
313.15	24.63	0.0007	0.0165	0.0050	25.82	−0.0009	0.0119	0.0080
316.15	25.42	−0.0076	0.0049	−0.0060	26.95	0.0034	0.0129	0.0109
319.15	26.94	0.0093	0.0153	0.0090	28.14	0.0079	0.0160	0.0136
323.15	28.16	−0.0033	0.0086	−0.0050	29.66	0.0083	0.0052	0.0111
326.15	29.25	−0.0089	0.0033	−0.0106	30.55	−0.0011	0.0023	−0.0008
329.15	31.05	0.0060	0.0176	0.0050	31.78	−0.0009	0.0008	−0.0035
333.15	32.84	0.0008	0.0123	0.0019	33.26	−0.0077	−0.0083	−0.0148
		$x_2=0.285$				$x_2=0.327$		
291.15	20.93	0.0168	−0.0002	0.0004	22.24	0.0159	0.0004	−0.0224
295.15	21.16	−0.0116	−0.0108	−0.0308	22.95	−0.0041	0.0040	−0.0275
299.15	22.15	−0.0083	−0.0115	−0.0287	23.73	−0.0219	0.0040	−0.0325
303.15	23.09	−0.0117	−0.0089	−0.0322	25.11	−0.0161	0.0029	−0.0162
306.15	24.41	0.0087	−0.0179	−0.0108	26.92	0.0161	0.0059	0.0220
309.15	24.90	−0.0084	−0.0226	−0.0269	27.41	−0.0032	0.0071	0.0077
313.15	26.54	0.0042	−0.0209	−0.0115	29.15	0.0088	0.0071	0.0242
316.15	27.75	0.0090	−0.0163	−0.0041	30.34	0.0119	0.0052	0.0293
319.15	28.44	−0.0074	−0.0214	−0.0177	31.05	−0.0016	0.0068	0.0172
323.15	30.78	0.0151	−0.0097	0.0098	32.40	−0.0075	0.0034	0.0113
326.15	31.95	0.0089	−0.0040	0.0077	33.97	0.0037	0.0014	0.0209
329.15	32.87	−0.0075	−0.0095	−0.0042	35.24	0.0045	0.0036	0.0195
333.15	34.89	−0.0088	0.0028	0.0013	36.51	−0.0075	−0.0002	0.0033

Standard uncertainties u are u (T)=0.05 K, u_r (p)=0.05, u_r (x_1)=0.02, u_r (x_2)=0.02

Table 2. Parameters of the modified Apelblat equation for $Fe(OTs)_3 \cdot 6H_2O$ in (ethanol+water) binary mixtures

Solvent	a	b	c	ARD
$x_2=0$	−9.46177	−1427.38	1.73708	0.0126
$x_2=0.050$	3.71833	−1811.84	−0.32099	0.0095
$x_2=0.099$	−112.341	3769.35	16.7859	0.0079
$x_2=0.147$	−130.634	4685.41	19.4697	0.0078
$x_2=0.193$	−146.979	5554.23	21.8454	0.0062
$x_2=0.239$	−65.2474	1784.13	9.72636	0.0063
$x_2=0.285$	−146.828	5554.75	21.8310	0.0097
$x_2=0.327$	−343.788	4011.42	51.4274	0.0094
			Overall ARD	0.0087

Table 1 and Fig. 4. Values of the average relative deviation (ARD) defined by Eq. (12) are also listed in Tables 2-4 [18].

$$\mathrm{ARD}=\frac{1}{N}\sum_{i=1}^{N}\frac{\left|x_i^{exp}-x_i^{cal}\right|}{x_i^{exp}} \tag{12}$$

in which N is the number of experimental points, and x_i^{exp} and x_i^{cal} are the experimental and calculation solubility values, respectively.

According to the corresponding results, the overall ARD for the modified Apelblat equation, the Redlich-Kister (CNIBS/R-K) model, and the hybrid model are 0.87%, 0.89%, and 1.61%, respectively, indicating that the experimental values are well-correlated with the three equations.

3. Thermodynamic Function of Solution

The standard molar enthalpy of solution obtained from the modified van't Hoff equation could be presented as follows [19]:

$$\Delta H_{soln}^{0}=-R\cdot\frac{\partial \ln x_1}{\partial(1/T)} \tag{13}$$

in which, R is gas constant.

Over a limited temperature interval, ΔH_{soln}^{0} would be valid for the mean temperature (T_{mean}). In this study, the value of T_{mean} is 312.08 K. Therefore, Eq. (13) can be presented as follows [20]:

$$\Delta H_{soln}^{0}=-R\cdot\frac{\partial \ln x_1}{\partial(1/T-1/T_{mean})} \tag{14}$$

Table 3. Parameters of the Redlich-Kister (CNIBS/R-K) model for $Fe(OTs)_3 \cdot 6H_2O$ in (ethanol+water) binary mixtures

T/K	A_1	A_2	A_3	A_4	A_5	ARD
291.15	−4.53715	4.41365	−4.00457	−32.8784	75.6924	0.0070
295.15	−4.37430	2.96455	−0.57147	−29.7867	63.7499	0.0092
299.15	−4.32169	2.92262	0.54375	−34.2428	66.4853	0.0105
303.15	−4.25274	2.66386	5.55377	−66.5765	124.906	0.0077
306.15	−4.18811	3.39255	−10.6686	15.9158	3.69291	0.0106
309.15	−4.10899	2.20605	1.99041	−35.1224	69.8715	0.0136
313.15	−4.04841	3.10822	−12.1470	28.7861	−19.0664	0.0134
316.15	−3.96582	2.26829	−5.40138	5.34204	9.99884	0.0093
319.15	−3.92530	2.13692	−1.97814	−12.8639	35.7619	0.0124
323.15	−3.83081	1.79507	−5.85476	24.0190	−35.2388	0.0064
326.15	−3.77464	1.99872	−6.50725	14.8016	−7.37672	0.0027
329.15	−3.73382	1.25939	3.91932	−30.8817	55.4087	0.0081
333.15	−3.65513	1.36978	1.77223	−23.1818	45.3439	0.0044
					Overall ARD	0.0089

Table 4. Parameters of the hybrid model for $Fe(OTs)_3 \cdot 6H_2O$ in (ethanol+water) binary mixtures

Parameters	Nonlinear regression values	
B_1	−44.5278	
B_2	326.921	
B_3	6.86341	
B_4	−213.380	
B_5	12113.8	
B_6	−799.374	
B_7	−4373.42	
B_8	11996.1	
B_9	30.8282	
	Overall ARD	0.0161

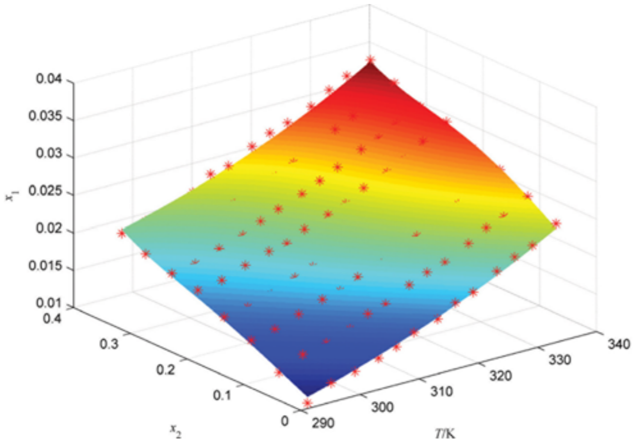

Fig. 4. Solubility of $Fe(OTs)_3 \cdot 6H_2O$ in (ethanol+water) binary mixtures obtained from hybrid model and the points are the experimental data.

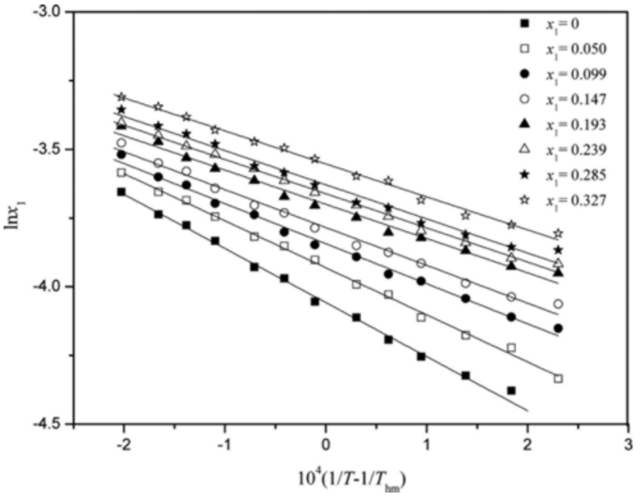

Fig. 5. Modified van't Hoff equation for $Fe(OTs)_3 \cdot 6H_2O$ in (ethanol+water) binary mixtures in mole fractions of ethanol, respectively.

Fig. 5 shows the plots of $\ln x_1$ versus $10^4(1/T-1/T_{mean})$ for $Fe(OTs)_3 \cdot 6H_2O$ in (ethanol+water) mixtures. From Fig. 5, it can be seen that the plots are linear and the values of the slope (k), the intercept (d) and the correlation coefficient (r^2) are listed in Table 5. Eq. (14) can be expressed as

$$\Delta H^0_{soln} = -R \cdot k \tag{15}$$

Based on the intercept (d) of the plots shown in Fig. 5, ΔG^0_{soln} can be calculated by Eq. (16) [21].

$$\Delta G^0_{soln} = -d \cdot R \cdot T_{mean} \tag{16}$$

ΔS^0_{soln} can be calculated through ΔH^0_{soln} and ΔG^0_{soln} by Eq. (17) [22].

$$\Delta S^0_{soln} = \frac{\Delta H^0_{soln} - \Delta G^0_{soln}}{T_{mean}} \tag{17}$$

The values of ΔH^0_{soln}, ΔG^0_{soln}, ΔS^0_{soln} for the dissolution process of $Fe(OTs)_3 \cdot 6H_2O$ in (ethanol+water) binary mixtures are also listed in Table 5.

The relative enthalpy (ζ_H) and entropy (ζ_{TS}) can be defined as the following equations [23,24]:

Table 5. Thermodynamic parameters for dissolution of $Fe(OTs)_3\cdot 6H_2O$ in (ethanol+water) binary mixtures at mean temperature

x_2	k	d	r^2	ΔH^0_{soln} kJ·mol^{-1}	ΔG^0_{soln} kJ·mol^{-1}	ΔS^0_{soln} J·mol^{-1}·K^{-1}	ζ_H	ζ_{TS}
0	−0.1968	−4.0575	0.9961	16.36	10.53	18.69	0.7372	0.2628
0.050	−0.1712	−3.9311	0.9975	14.23	10.20	12.92	0.7793	0.2207
0.099	−0.1457	−3.8433	0.9936	12.11	9.97	6.86	0.8498	0.1502
0.147	−0.1377	−3.7844	0.9909	11.45	9.82	5.22	0.8755	0.1245
0.193	−0.1247	−3.7000	0.9877	10.37	9.60	2.46	0.9310	0.0690
0.239	−0.1244	−3.6613	0.9955	10.35	9.50	2.71	0.9245	0.0755
0.285	−0.1242	−3.6289	0.9855	10.33	9.42	2.93	0.9188	0.0812
0.327	−0.1200	−3.5530	0.9944	9.98	9.22	2.44	0.9291	0.0709

Table 6. Thermodynamic functions of the transfer of $Fe(OTs)_3\cdot 6H_2O$ from more polar solvents to less polar ones to the solution in (ethanol+water) binary mixtures at 312.08 K

x_2		$\Delta_{A\to B}H^0_{soln}$ kJ·mol^{-1}	$\Delta_{A\to B}G^0_{soln}$ kJ·mol^{-1}	$\Delta_{A\to B}S^0_{soln}$ J·mol^{-1}·K^{-1}	$T\Delta_{A\to B}S^0_{soln}$ kJ·mol^{-1}
A	B				
0	0.050	−2.13	−0.33	−5.77	−1.80
0.050	0.099	−2.12	−0.23	−6.05	−1.89
0.099	0.147	−0.67	−0.15	−1.65	−0.51
0.147	0.193	−1.08	−0.22	−2.75	−0.86
0.193	0.239	−0.02	−0.10	0.24	0.08
0.239	0.285	−0.02	−0.08	0.22	0.07
0.285	0.327	−0.35	−0.20	−0.49	−0.15

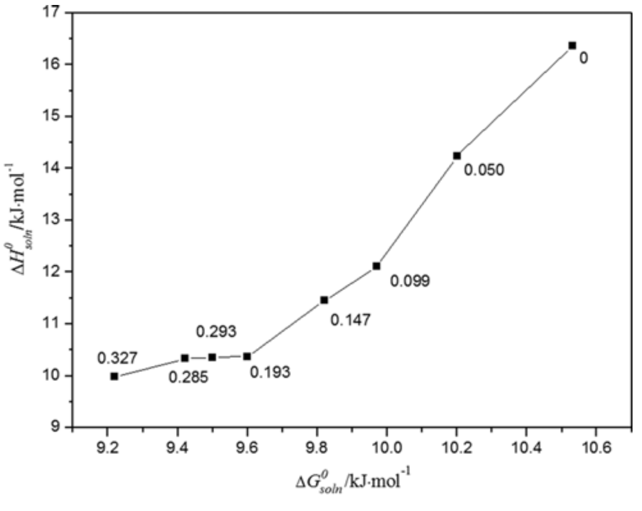

Fig. 6. ΔH^0_{soln} versus ΔG^0_{soln} enthalpy-entropy compensation plot for the dissolution process of $Fe(OTs)_3\cdot 6H_2O$ in (ethanol+water) binary mixtures at 312.08 K.

$$\zeta_H = \frac{|\Delta H^0_{soln}|}{|\Delta H^0_{soln}| + |T_{mean}\,\Delta S^0_{soln}|} \tag{18}$$

$$\zeta_{TS} = \frac{|T_{mean}\,\Delta S^0_{soln}|}{|\Delta H^0_{soln}| + |T_{mean}\,\Delta S^0_{soln}|} \tag{19}$$

The values of ζ_H and ζ_{TS} were calculated and also listed in Table 5. From Table 5, we can see that the ΔH^0_{soln} and ΔG^0_{soln} values are observed as positive values in the investigated solvents, indicating that the dissolution of $Fe(OTs)_3\cdot 6H_2O$ in the solvents was endothermic and spontaneous. Moreover, the main contributor to the standard Gibbs energy of solution was enthalpy during the dissolution, because of the values of $\zeta_H>0.7$.

4. Enthalpy-entropy Compensation

The increasing mole fraction of the solvent mixtures was regarded as ethanol being gradually added to the water; the polarity of the solvent decreases continuously with an increase in the composition of solvent mixtures in this experiment. The thermodynamic functions of transfer ($\Delta_{A\to B}H^0_{soln}$, $\Delta_{A\to B}G^0_{soln}$ and $\Delta_{A\to B}S^0_{soln}$) of $Fe(OTs)_3\cdot 6H_2O$ from polar solvents to the less polar ones can be calculated from the data shown in Table 5, and the results are listed in Table 6. According to Table 6, the dissolution process is driven by the enthalpy when x_2 changes from 0 to 0.193 and 0.285 to 0.327 ($\Delta_{A\to B}H^0_{soln}<0$, $\Delta_{A\to B}G^0_{soln}<0$, and $\Delta_{A\to B}S^0_{soln}<0$), and when x_2 changes from 0.193 to 0.285 ($\Delta_{A\to B}H^0_{soln}<0$, $\Delta_{A\to B}G^0_{soln}<0$, and $\Delta_{A\to B}S^0_{soln}>0$).

Some physicochemical compensation effects for the solubility of several drugs in aqueous solvent mixtures were demonstrated by Bustamante et al. [25]. The weighted graphs of ΔH^0_{soln} as a function of ΔG^0_{soln} at T_{mean} were used to identify the mechanism of the co-solvent action [26-29]. Fig. 6 shows the plots of ΔH^0_{soln} versus ΔG^0_{soln} for the dissolution of $Fe(OTs)_3\cdot 6H_2O$ in (ethanol+water) binary mixtures. From Fig. 6, the non-linear curve has a variable positive slop when x_2 changes from 0 to 0.327. In this case, the driving mechanism for solubility is the enthalpy probably due to better solvation of the drug by ethanol molecules.

CONCLUSIONS

The solubility data of $Fe(OTs)_3·6H_2O$ in (ethanol+water) binary mixtures were measured at temperatures ranging from 291.15 to 333.15 K. The mole fraction of ethanol was 0, 0.050, 0.099, 0.147, 0.193, 0.239, 0.285 and 0.327. The experimental data were correlated by the modified Apelblat equation, the Redlich-Kister (CNIBS/R-K) model, and the hybrid model with good consequences (overall ARD<1.7%). In addition, the thermodynamic parameters (ΔH^0_{soln}, ΔG^0_{soln}, ΔS^0_{soln}) for the dissolution process of $Fe(OTs)_3·6H_2O$ in (ethanol+water) binary mixtures at mean harmonic temperature were obtained by a modified van't Hoff equation. The results showed that the dissolution process of $Fe(OTs)_3·6H_2O$ is endothermic and spontaneous. The thermodynamic functions of transfer ($\Delta_{A\rightarrow B}H^0_{soln}$, $\Delta_{A\rightarrow B}G^0_{soln}$, and $\Delta_{A\rightarrow B}S^0_{soln}$) of $Fe(OTs)_3·6H_2O$ from polar solvents to the less polar ones can be calculated, and the results showed that the driving mechanism is the enthalpy ($0<x_2<0.327$).

NOMENCLATURE

A_1, A_2, A_3, A_4 and A_5 : parameters of the Redlich-Kister (CNIBS/R-K) model
a, b and c : parameters of the modified Apelblat equation
B_1 to B_9 : parameters of the hybrid model
d : intercept
J_i : parameters of the hybrid model
k : slope
m_1 : the mass of the $Fe(OTs)_3·6H_2O$ [g]
m_2 : the mass of the ethanol [g]
m_3 : the mass of the water [g]
M_1 : the molecular mass of $Fe(OTs)_3·6H_2O$ [g/mol]
M_2 : the molecular mass of ethanol [g/mol]
M_3 : the molecular mass of water [g/mol]
n : the number of the solvents
N : the number of experiment points
p : pressure [Mpa]
R : gas constant [8.314 $J·mol^{-1}·K^{-1}$]
r^2 : the correlation coefficient
T : temperature [K]
T_{mean} : the mean temperature [K]
x_1 : the mole fraction of the solute
x_2 : the mole fraction of the solvent
ΔH^0_{soln} : enthalpy of the dissolution process [kJ/mol]
ΔS^0_{soln} : entropy of the dissolution process [$J·mol^{-1}·K^{-1}$]
ΔG^0_{soln} : standard mole Gibbs free energy of the dissolution process [kJ/mol]

Greek Letters

ζ_H : the relative enthalpy
ζ_{TS} : the relative entropy

Abbreviations

HPLC : high performance liquid chromatography
TGA : thermal gravity analysis
IR : infrared spectroscopy
ARD : average relative deviation
SI : supporting information

Superscripts

B : ethanol
C : water
exp : experimental
cal : calculated

SUPPORTING INFORMATION

Additional information as noted in the text. This information is available via the Internet at http://www.springer.com/chemistry/journal/11814.

REFERENCES

1. M. Horacio and M. M. Afonso, *Synth Commun.*, **38**, 2607 (2008).
2. M. J. Spafford, E. D. Anderson, J. R. Lacey, A. C. Palma and R. S. Mohan, *Tetrahedron. Lett.*, **48**, 8665 (2007).
3. K. Komeyama, T. Morimoto, Y. Nakayama and K. Takaki, *Tetrahedron. Lett.*, **48**, 3259 (2007).
4. F. Ke, Z. K. Li, H. F. Xiang and X. G. Zhou, *Tetrahedron. Lett.*, **52**, 318 (2011).
5. J. C. Choi, K. Kohno, D. Masuda, H. Yasuda and T. Sakakura, *Chem. Commun.*, **38**, 777 (2008).
6. M. S. Jung, W. S. Kim, Y. H. Shin, H. J. Jin, Y. S. Kim and E. J. Kang, *Org. Lett.*, **14**, 6262 (2012).
7. J. M. Bothwell, V. V. Angeles, J. P. Carolan, M. E. Olson and R. S. Mohan, *Tetrahedron. Lett.*, **51**, 1056 (2010).
8. M. E. Olson, J. P. Carolan, M. V. Chiodo, P. R. Lazzara and R. S. Mohan, *Tetrahedron. Lett.*, **51**, 3969 (2010).
9. S. M. Holmes, S. G. Mckinley and G. S. Girolami, *Inorganic Syntheses.*, **33**, 91 (2002).
10. J. Chen, Z. X. Zeng, W. L. Xue, D. Wang and Y. Huang, *Ind. Eng. Chem. Res.*, **50**, 11755 (2011).
11. C. Yu, Z. X. Zeng and W. L. Xue, *Ind. Eng. Chem., Res.*, **54**, 3961 (2015).
12. C. Yu, Z. J. Huang, Z. X. Zeng and W. L. Xue, *J. Solution Chem.*, **45**, 395 (2016).
13. A. Apelblat and E. Manzurola, *J. Chem. Thermodynamics*, **31**, 85 (1999).
14. A. Apelblat and E. Manzurola, *Chem. Thermodyn.*, **33**, 147 (2001).
15. Q. H. Luan, Y. L. Wang, G. Wang, J. X. Yang and H. X. Hao, *J. Chem. Eng. Data*, **59**, 2642 (2014).
16. A. Jouyban-Gharamaleki and W. E. Acree Jr., *Int. J. Pharm.*, **167**, 177 (1998).
17. Z. M. Zhou, Y. X. Qu, J. D. Wang, S. Wang, J. S. Liu and M. Wu, *J. Chem. Eng. Data*, **56**, 1622 (2011).
18. M. M. Liang, Y. H. Hu, X. Liu, J. Guan, W. G. Yang and Y. Liu, *J. Mol. Liq.*, **197**, 35 (2014).
19. X. Q. Zhou, J. S. Fan, N. Li, Z. X. Du, H. J. Ying, J. L. Wu, J. Xiong and J. X. Bai, *Fluid Phase Equilib.*, **316**, 26 (2012).
20. D. M. Cristancho and F. Martínez, *J. Mol. Liq.*, **200**, 122 (2014).
21. D. W. Wei, H. L. Li, Y. N. Li and J. Zhu, *Fluid Phase Equilib.*, **316**, 132 (2012).
22. A. Maher, D. Croker, A. C. Rasmuson and B. K. Hodnett, *J. Chem.*

Eng. Data, **55**, 5314 (2010).

23. Y. Yang, Q. Zhang, C. C. Cao, L. M. Cheng, Y. Shi, W. G. Yang and Y. H. Hu, *Thermochim. Acta*, **592**, 52 (2014).
24. A. R. Holguín, D. R. Delgado, F. Martínez and Y. Marcus, *J. Solution Chem.*, **40**, 1987 (2011).
25. M. A. Ruidiaz, D. R. Delgado, F. Martínez and Y. Marcus, *Fluid Phase Equilib.*, **299**, 259 (2010).
26. E. Tomlinson, *Int. J. Pharm.*, **13**, 115 (1983).
27. E. A. Ahumada, D. R. Delgado and F. Martínez, *Fluid Phase Equilib.*, **332**, 120 (2012).
28. J. Y. Zhang, P. P. Zhang, T. T. Liu, L. Zhou, L. Q. Zhang, R. Lin, G. D. Yang, W. R.Wang and Y. P. Li, *J. Mol. Liq.*, **203**, 98 (2015).
29. D. R. Delgado, G. A. Rodríguez and F. Martínez, *J. Mol. Liq.*, **177**, 156 (2013).

Supporting Information

Solubility and dissolution thermodynamics of hexaquoiron(III)tris(*p*-toluenesulfonate) in (ethanol+water) binary mixtures within 291.15-333.15 K

Zhijuan Huang, Chao Yu, Weilan Xue, Fucong Lin, and Zuoxiang Zeng[†]

Institute of Chemical Engineering, East China University of Science and Technology, Shanghai 200237, China

(*Received 5 May 2016 • accepted 29 August 2016*)

The procedure of the pre-experiment

The procedure of the pre-experiment was briefly described as follows. Firstly, a set of binary mixtures with the initial mole fractions of ethanol ($x_2'^0$=0, 0.057, 0.114, 0.171, 0.228, 0.285, 0.342, 0.399) were prepared, than the solubility of $Fe(OTs)_3 \cdot 6H_2O$ at different temperature T=(291.15 to 333.15 K) was measured by the last crystal disappearance method. The final mole fractions of ethanol (x_2) at different temperatures is calculated according to Eq. (2) described in the text, and the arithmetic average value (x_2^{av}) of x_2 was calculated. The relative deviation (RD) between x_2^{av} and x_2 defined by Eq. (S1).

$$RD=\frac{x_2^{av}-x_2}{x_2^{av}}\times 100\% \qquad (S1)$$

The values of $x_2'^0$, x_2, x_2^{av}, and RD were listed in Table S1. According to the values of x_2^{av} and RD, a new initial mole fraction of ethanol (x_2^0) can be obtained to make x_2 be approximate to x_2^{av} at a specified temperature. According to the values of x_2^0 at different temperatures, a set of (ethanol+water) binary mixtures were prepared to measured the solubility of $Fe(OTs)_3 \cdot 6H_2O$ with different mole fractions of ethanol (x_2=0, 0.050, 0.099, 0.147, 0.193, 0.239, 0.285, 0.327) from T=(291.15 to 333.15) K. The comparisons between experimental data (x_2) and calculated ones (x_2^{av}) can be indicated by the relative deviation (RD′) defined by Eq. (S2).

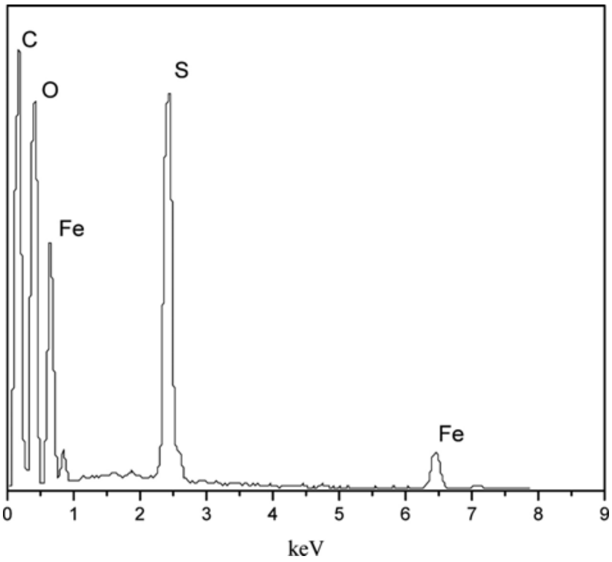

Fig. S1. Energy disperse spectroscope image of $Fe(OTs)_3 \cdot 6H_2O$.

$$RD'=\frac{x_2^{av}-x_2}{x_2^{av}}\times 100\% \qquad (S2)$$

The values of x_2^0, x_2, x_2^{av} and RD′ are shown in Table (S2). From

Table S1. The values of $x_2'^0$, x_2, x_2^{av}, and RD at temperature T

T/K	$x_2'^0$	x_2	RD	$x_2'^0$	x_2	RD	$x_2'^0$	x_2	RD	$x_2'^0$	x_2	RD
	x_2^{av}=0				x_2^{av}=0.050			x_2^{av}=0.099			x_2^{av}=0.147	
291.15	0	0	0	0.057	0.052	−4.91%	0.114	0.103	−4.10%	0.171	0.153	−4.11%
295.15	0	0	0	0.057	0.052	−3.81%	0.114	0.103	−3.63%	0.171	0.153	−3.79%
299.15	0	0	0	0.057	0.052	−3.34%	0.114	0.102	−2.81%	0.171	0.152	−3.14%
303.15	0	0	0	0.057	0.051	−2.61%	0.114	0.101	−1.99%	0.171	0.150	−2.13%
306.15	0	0	0	0.057	0.051	−1.60%	0.114	0.101	−1.65%	0.171	0.149	−1.53%
309.15	0	0	0	0.057	0.051	−1.13%	0.114	0.100	−0.75%	0.171	0.149	−1.15%
313.15	0	0	0	0.057	0.050	0.10%	0.114	0.099	−0.09%	0.171	0.147	−0.13%
316.15	0	0	0	0.057	0.050	0.85%	0.114	0.098	0.64%	0.171	0.146	0.81%
319.15	0	0	0	0.057	0.049	1.37%	0.114	0.097	1.70%	0.171	0.145	1.30%
323.15	0	0	0	0.057	0.049	2.56%	0.114	0.097	2.43%	0.171	0.143	2.46%
326.15	0	0	0	0.057	0.048	3.60%	0.114	0.095	3.67%	0.171	0.142	3.69%
329.15	0	0	0	0.057	0.048	4.17%	0.114	0.095	4.24%	0.171	0.141	4.31%
333.15	0	0	0	0.057	0.047	5.53%	0.114	0.093	5.96%	0.171	0.138	5.94%

Table S1. Continued

T/K	$x_2^{\prime 0}$	x_2	RD	$x_2^{\prime 0}$	x_2	RD	$x_2^{\prime 0}$	x_2	RD	$x_2^{\prime 0}$	x_2	RD
	$x_2^{av}=0.193$				$x_2^{av}=0.239$			$x_2^{av}=0.285$			$x_2^{av}=0.327$	
291.15	0.228	0.201	−4.24%	0.285	0.250	−4.73%	0.342	0.298	−4.61%	0.399	0.345	−5.37%
295.15	0.228	0.200	−3.88%	0.285	0.250	−4.41%	0.342	0.298	−4.43%	0.399	0.343	−4.82%
299.15	0.228	0.199	−3.03%	0.285	0.247	−3.52%	0.342	0.296	−3.69%	0.399	0.341	−4.22%
303.15	0.228	0.197	−2.27%	0.285	0.246	−2.82%	0.342	0.294	−2.98%	0.399	0.337	−3.17%
306.15	0.228	0.197	−1.96%	0.285	0.244	−1.92%	0.342	0.291	−1.98%	0.399	0.333	−1.76%
309.15	0.228	0.195	−1.02%	0.285	0.242	−1.16%	0.342	0.290	−1.62%	0.399	0.332	−1.39%
313.15	0.228	0.193	−0.24%	0.285	0.240	−0.29%	0.342	0.286	−0.37%	0.399	0.327	−0.04%
316.15	0.228	0.192	0.36%	0.285	0.238	0.57%	0.342	0.283	0.55%	0.399	0.324	0.89%
319.15	0.228	0.190	1.49%	0.285	0.235	1.47%	0.342	0.282	1.08%	0.399	0.322	1.44%
323.15	0.228	0.188	2.40%	0.285	0.233	2.62%	0.342	0.277	2.86%	0.399	0.319	2.50%
326.15	0.228	0.187	3.22%	0.285	0.229	4.06%	0.342	0.274	3.76%	0.399	0.315	3.73%
329.15	0.228	0.184	4.58%	0.285	0.227	4.90%	0.342	0.272	4.47%	0.399	0.312	4.72%
333.15	0.228	0.182	5.93%	0.285	0.225	5.83%	0.342	0.268	6.03%	0.399	0.308	5.73%

Table S2. The values of x_2^0, x_2, x_2^{av} and RD′ at temperature *T*

T/K	x_2^0	x_2	RD′	x_2^0	x_2	RD′	x_2^0	x_2	RD′	x_2^0	x_2	RD′
		$x_2^{av}=0$			$x_2^{av}=0.050$			$x_2^{av}=0.099$			$x_2^{av}=0.147$	
291.15	0	0	0	0.054	0.0499	−0.24%	0.109	0.0988	−0.17%	0.164	0.1468	−0.17%
295.15	0	0	0	0.055	0.0499	−0.15%	0.110	0.0989	−0.13%	0.165	0.1468	−0.14%
299.15	0	0	0	0.055	0.0499	−0.11%	0.111	0.0989	−0.08%	0.166	0.1469	−0.10%
303.15	0	0	0	0.056	0.0500	−0.07%	0.112	0.0990	−0.04%	0.167	0.1469	−0.05%
306.15	0	0	0	0.056	0.0500	−0.03%	0.112	0.0990	−0.03%	0.168	0.1470	−0.02%
309.15	0	0	0	0.056	0.0500	−0.01%	0.113	0.0990	−0.01%	0.169	0.1470	−0.01%
313.15	0	0	0	0.057	0.0500	0.00%	0.114	0.0990	0.00%	0.171	0.1470	0.00%
316.15	0	0	0	0.057	0.0500	−0.01%	0.115	0.0990	0.00%	0.172	0.1470	−0.01%
319.15	0	0	0	0.058	0.0500	−0.02%	0.116	0.0990	−0.03%	0.173	0.1470	−0.02%
323.15	0	0	0	0.058	0.0500	−0.07%	0.117	0.0989	−0.06%	0.175	0.1469	−0.06%
326.15	0	0	0	0.059	0.0499	−0.13%	0.118	0.0989	−0.13%	0.177	0.1468	−0.14%
329.15	0	0	0	0.059	0.0499	−0.17%	0.119	0.0988	−0.18%	0.178	0.1467	−0.19%
333.15	0	0	0	0.060	0.0498	−0.31%	0.121	0.0986	−0.36%	0.181	0.1465	−0.35%
	$x_2^{av}=0.193$				$x_2^{av}=0.239$			$x_2^{av}=0.285$			$x_2^{av}=0.327$	
291.15	0.218	0.1927	−0.18%	0.272	0.2385	−0.22%	0.326	0.2844	−0.21%	0.378	0.3261	−0.29%
295.15	0.219	0.1927	−0.15%	0.272	0.2385	−0.19%	0.327	0.2844	−0.20%	0.380	0.3262	−0.23%
299.15	0.221	0.1928	−0.09%	0.275	0.2387	−0.12%	0.329	0.2846	−0.14%	0.382	0.3264	−0.18%
303.15	0.223	0.1929	−0.05%	0.277	0.2388	−0.08%	0.332	0.2847	−0.09%	0.386	0.3267	−0.10%
306.15	0.224	0.1929	−0.04%	0.280	0.2389	−0.04%	0.335	0.2849	−0.04%	0.392	0.3269	−0.03%
309.15	0.226	0.1930	−0.01%	0.282	0.2390	−0.01%	0.336	0.2849	−0.03%	0.393	0.3269	−0.02%
313.15	0.227	0.1930	0.00%	0.284	0.2390	0.00%	0.341	0.2850	0.00%	0.399	0.3270	0.00%
316.15	0.229	0.1930	0.00%	0.287	0.2390	0.00%	0.344	0.2850	0.00%	0.403	0.3270	−0.01%
319.15	0.231	0.1930	−0.02%	0.289	0.2389	−0.02%	0.346	0.2850	−0.01%	0.405	0.3269	−0.02%
323.15	0.233	0.1929	−0.06%	0.292	0.2388	−0.07%	0.352	0.2848	−0.08%	0.409	0.3268	−0.06%
326.15	0.235	0.1928	−0.10%	0.297	0.2386	−0.17%	0.355	0.2846	−0.14%	0.414	0.3265	−0.14%
329.15	0.238	0.1926	−0.21%	0.299	0.2384	−0.24%	0.357	0.2844	−0.20%	0.418	0.3263	−0.22%
333.15	0.242	0.1923	−0.35%	0.302	0.2382	−0.34%	0.363	0.2840	−0.36%	0.422	0.3259	−0.33%

Table (S2), the absolute values of RD′ are less than 0.36% which meas this method has promising feasibility and efficiency.